

An Occurrence of Metastable Cristobalite in High-Pressure Garnet Granulite

Robert S. Darling, I-Ming Chou, Robert J. Bodnar

High-pressure (0.8 gigapascals) granulite facies garnet from Gore Mountain, New York, hosts multiple solid inclusions containing the low-pressure silica polymorph cristobalite along with albite and minor ilmenite. Identification of cristobalite is based on Raman spectra, electron microprobe analysis, and microthermometric measurements on the α/β phase transformation. The cristobalite plus albite inclusions may have originated as small, trapped samples of hydrous sodium–aluminum–siliceous melt. Diffusive loss of water from these inclusions under isothermal, isochoric conditions may have resulted in a large enough internal pressure decrease to promote the metastable crystallization of cristobalite.

Cristobalite is a low-density SiO_2 polymorph. Its high-temperature form (β -cristobalite) is cubic and is stable between 1470° and 1728°C at a pressure of 1 atm (1). However, it can persist metastably to much lower temperatures, and at $\sim 250^\circ\text{C}$ experiences a displacive phase transformation to a tetragonal form (α -cristobalite). Cristobalite has been described from low-pressure environments, such as volcanic rocks of various composition (1), fulgarites (1), deep-sea cherts (2), shallow-contact metamorphic rocks (3), and low-temperature, hydrothermal precipitates (4). In most of these cases, cristobalite forms metastably, at temperatures below its stability field. Here, we describe and interpret an occurrence of cristobalite in high-pressure (0.8 GPa), granulite facies garnet from a Middle Proterozoic (1.06×10^9 years ago) metabasite.

The cristobalite occurs inside the large, almandine-pyrope garnets of the Barton Mine on the north slope of Gore Mountain, in the south-central Adirondack Highlands of New York. It occurs exclusively in multiple solid inclusions containing albite and a minor amount of platy, hexagonal ilmenite. The cristobalite contains numerous fractures, the number of which is directly related to crystal volume. Many of the cristobalite-bearing inclusions are elongated, rod- or bladellike; others are irregular or circular (Fig. 1). The largest bladellike inclusions range from 3 to 10 μm in width, 20 to 80 μm in length, and 2 to 4 μm thick. Each inclusion has a relatively consistent phase ratio approximating 50 to 65% by volume cristobalite, 30 to 45% albite, and 5% ilmenite (Fig. 1). The inclusions are widely disseminated in garnet and are interpreted to be of primary origin. Other solid

and multiple solid inclusions in Gore Mountain garnet include (i) albite + ilmenite, (ii) albite, (iii) ilmenite, and (iv) rutile.

We identified cristobalite by observing its phase behavior as inclusions were heated through the α/β transformation. Between 260° and 270°C, the fractures in cristobalite sequentially closed, with each fracture closing instantly. After closure, the fractures were nearly invisible (Fig. 1). The closing of fractures is attributed to the 5% volume increase associated with the displacive phase transformation to β -cristobalite (5). Also, in high-intensity, cross-polarized light, the thickest cristobalites (3 to 4 μm) showed an instant change from first-order dark gray (weakly anisotropic) to black (isotropic), a characteristic of the tetragonal (α) to cubic (β) transformation. Upon cooling, the same fractures reopened between 240° and 250°C. This hysteresis is also characteristic of the β -to α -cristobalite phase transformation (6, 7). Hysteresis measurements on 24 cristobalites averaged $19.5^\circ \pm 2.9^\circ\text{C}$ (1σ), a value in agreement with experimental data (6). The transformation temperatures also indicate that pressure inside the inclusion was less than 0.01 GPa (8).

We also analyzed the composition of the inclusions by electron microprobe. However, because the cristobalite is small and of low density, it was nearly impossible to obtain an analysis that was not affected to some extent by the surrounding garnet, even at accelerating voltages as low as 8 kV. Our best analysis yielded 97.0% SiO_2 and 0.23% Al_2O_3 by weight. No K_2O , Na_2O , or TiO_2 was detected. Additionally, the albite composition was 70.1% SiO_2 , 18.0% Al_2O_3 , 2.4% Fe_2O_3 , 0.9% CaO , and 7.2% Na_2O by weight. No K_2O was detected. The values deviate slightly from stoichiometric albite, which we attribute to Na loss during analysis. The structural state of the albite is unknown. The oxide phase was too small (0.5 to 1.0 μm across) to

obtain a quantitative analysis, but the energy dispersive x-ray fluorescence spectra showed strong Fe and Ti peaks, which are consistent with ilmenite.

The cristobalite was also verified by laser Raman microspectrometry (Fig. 2). The cristobalite in Gore Mountain garnet shows characteristic peaks at 112.0, 229.9, 285.5, 417.2, and 781.2 cm^{-1} , values which are within error of those determined for natural cristobalite (109.0, 226.9, 413.3, 782.0 cm^{-1}) (Fig. 2) and synthetic polycrystalline cristobalite (110, 230, 275, 287, 416, 785 cm^{-1}) (Fig. 2) at 25°C (9).

The occurrence of cristobalite in granulite facies garnet raises two questions. First, did the cristobalite form within its stability field or at granulite facies? Second, if formed under the latter conditions, what mechanism could allow for the formation of a low-density silica polymorph? The exceptionally large (10 to 100 μm across) garnet hosts at Gore Mountain are thought to have formed as a result of porphyroblastic growth aided by the local influx of water (source unknown) into an olivine gabbro protolith (10). The added water reacted with orthopyroxene, olivine, and plagioclase to form garnet, par-

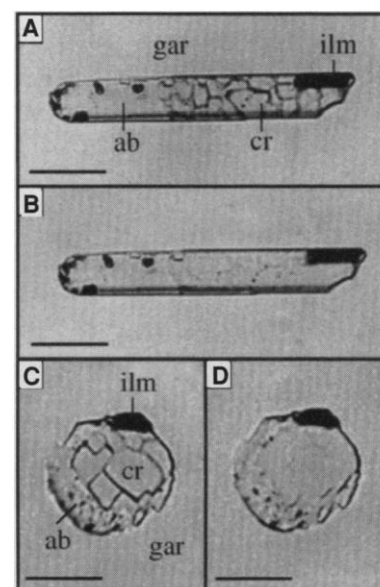


Fig. 1. Photomicrographs of multiple solid inclusions in Gore Mountain garnet (gar). (A) Large bladellike inclusion containing albite (ab), α -cristobalite (cr), and ilmenite (ilm) at 260°C; highly fractured cristobalite is apparent. (B) The same inclusion at 275°C, showing the closing of fractures after transforming to β -cristobalite. The Raman spectrum in Fig. 2A is derived from the cristobalite shown in (A) and (B). (C) Large circular inclusion containing the same phases at 260°C; similar fractures are apparent in α -cristobalite. (D) The same inclusion at 275°C; a similar closing of fractures is apparent. Dark spots in albite are unidentified. Bar, 20 μm .

R. S. Darling, Department of Geology, State University of New York College at Cortland, Cortland, NY 13045, USA. I.-M. Chou, U.S. Geological Survey, 955 National Center, Reston, VA 20192, USA.

R. J. Bodnar, Department of Geological Sciences, 4044 Derring Hall, Virginia Polytechnic Institute and State University, Blacksburg, VA 24061, USA.

case where internal (inclusion) pressure is lower than external (confining) pressure (21). Our melt interpretation no doubt needs further testing, but we believe it is the most plausible explanation as compared to other hypotheses (22).

It is remarkable that the cristobalite was able to resist reconstructive transformation to β -quartz during denudation and cooling of the rock, considering that the Adirondack Highlands cooled at a rate of -1.5°C per million years after the peak of granulite facies metamorphism, staying at temperatures in excess of 600°C for 100 million years (23). The cristobalite may have survived because of the absence of water, which serves to catalyze reconstructive transformation. Water may not have had access to these rocks until mid- to upper-levels of the crust were reached during uplift, but it is unlikely that significant diffusion of water back into the garnets occurred at these temperatures. The absence of water was also suggested to explain the preservation of coesite inclusions in garnet (and other phases) from ultra-high-pressure rocks (24, 25). The preservation of cristobalite in rocks cooled slowly from high temperature implies that, in the absence of water, the activation energy for the β -cristobalite to β -quartz transformation is high.

REFERENCES AND NOTES

1. C. Frondel, *The System of Mineralogy*, vol. 3, *Silica Minerals* (Wiley, New York, ed. 7, 1962).
2. J. A. Klasik, *Science* **189**, 631 (1975).
3. D. S. Beljankin and V. P. Petrov, *Am. Mineral.* **23**, 153 (1938).
4. A. Van Valkenburg and B. F. Buie, *ibid.* **30**, 526 (1945).
5. W. W. Schmahl, I. P. Swainson, M. T. Dove, A. Graeme-Barber, *Z. Kristallogr.* **201**, 125 (1992).
6. W. W. Schmahl, *Eur. J. Mineral.* **5**, 377 (1993).
7. V. G. Hill and R. Roy, *J. Am. Ceram. Soc.* **41**, 532 (1958).
8. L. H. Cohen and W. Klement Jr., *Philos. Mag. A* **39**, 399 (1979).
9. J. B. Bates, *J. Chem. Phys.* **57**, 4042 (1972).
10. D. de Waard, *J. Petrol.* **8**, 210 (1967); F. Luther, thesis, Lehigh University, Bethlehem, PA (1976).
11. R. G. Berman, *J. Petrol.* **29**, 445 (1988).
12. A. E. Ringwood and D. H. Green, *Tectonophysics* **3**, 383 (1966).
13. J. R. Holloway, *Geochim. Cosmochim. Acta* **37**, 651 (1973).
14. S. R. Bohlen *et al.*, *J. Petrol.* **26**, 971 (1985).
15. F. S. Spear and J. C. Markussen, *ibid.*, in press.
16. K. R. Hosieni *et al.*, *Am. Mineral.* **70**, 782 (1985).
17. S. Wen and H. Nekvasil, *ibid.* **79**, 316 (1994).
18. If this process occurred at $T \geq 910^{\circ}\text{C}$, the melt would enter the tridymite stability field.
19. J. F. Schairer and N. L. Bowen, *Am. J. Sci.* **254**, 129 (1956).
20. L. Wang *et al.*, *Am. Mineral.* **81**, 706 (1996).
21. S. M. Sterner and R. J. Bodnar, *J. Metamorphic Geol.* **7**, 243 (1989); M. O. Vityk, R. J. Bodnar, V. Dudok, *Eur. J. Mineral.* **7**, 1071 (1995).
22. Other possible interpretations include (i) a garnet + β -cristobalite epitaxial relation, (ii) a devitrification product of glass inclusions, or (iii) an exsolution product of supersilicic garnet.
23. K. Mezger, C. M. Rawnsley, S. R. Bohlen, G. N.

- Hanson, *J. Geol.* **99**, 415 (1991).
24. C. Chopin, *Contrib. Mineral. Petrol.* **86**, 107 (1984); A. I. Okay, X. Shutong, A. M. C. Sengör, *Eur. J. Mineral.* **1**, 595 (1989); X. Wang, J. G. Liou, H. K. Mao, *Geology* **17**, 1085 (1989).
25. Unlike these occurrences of coesite, we did not observe marginal- or fracture-related replacement of cristobalite by α -quartz. The reason for this is unknown, but the two polymorphs did experience very different retrograde *PT* paths, which will affect the availability and diffusivity of water, as well as the compressibility and expansivity of the host

- and inclusion phases.
26. We thank D. Lindsley, F. Florence, and H. Nekvasil for help with this investigation, J. Ireland for technical assistance, B. Gravatt and J. Hunt for assistance in scanning electron microscopy and electron microprobe analysis, and P. Dunn and J. Post of the Smithsonian Institution for providing natural cristobalite for Raman analysis. Suggestions by P. Barton, G. Nord, and two anonymous reviewers greatly improved earlier versions of this manuscript.

30 October 1996; accepted 30 January 1997

Spatial Variability of Turbulent Mixing in the Abyssal Ocean

K. L. Polzin,* J. M. Toole, J. R. Ledwell, R. W. Schmitt

Ocean microstructure data show that turbulent mixing in the deep Brazil Basin of the South Atlantic Ocean is weak at all depths above smooth abyssal plains and the South American Continental Rise. The diapycnal diffusivity there was estimated to be less than or approximately equal to 0.1×10^{-4} meters squared per second. In contrast, mixing rates are large throughout the water column above the rough Mid-Atlantic Ridge, and the diffusivity deduced for the bottom-most 150 meters exceeds 5×10^{-4} meters squared per second. Such patterns in vertical mixing imply that abyssal circulations have complex spatial structures that are linked to the underlying bathymetry.

An outstanding question in oceanography is the intensity and spatial distribution of turbulent vertical mixing in the deep sea. Beyond affecting the dispersal of naturally occurring and anthropogenic substances, mixing relates through the buoyancy (heat) equation (1) and vorticity dynamics (2) to the intensity of upwelling and the horizontal circulation in the abyss. The rate of turbulent mixing at depth has previously been inferred from advective heat budgets constructed for deep, semi-enclosed basins (3, 4). These studies report vertical diffusivity values (*K*) between 1×10^{-4} and $10 \times 10^{-4} \text{ m}^2 \text{ s}^{-1}$: one to two orders of magnitude greater than values deduced for the upper ocean interior from ocean microstructure data (5) and a tracer experiment (6), and from limited deep observations away from boundaries (5, 7, 8). Those few deep-ocean microstructure observations near rough bathymetry suggest that mixing there is much enhanced (8, 9). To further examine the intensity, spatial distribution, and mechanisms of mixing in the deep ocean, we initiated a joint physical oceanographic and tracer study in the Brazil Basin of the South Atlantic Ocean. This area was chosen because a diffusivity estimate based on an abyssal heat budget was available for this region (3) and extensive data have recently been collected there as part of the

World Ocean Circulation Experiment.

We made physical observations with a freely falling instrument, the High Resolution Profiler (HRP) (10). This device returns temperature, salinity, and horizontal velocity information as a function of depth, along with dissipation estimates of turbulent kinetic energy and temperature variance. We infer turbulent diffusivity from the dissipation estimates, using models that assume a balance between turbulent production and dissipation (11). An independent technique we used to study mixing involves tracking an inert chemical tracer that is injected on a deep density surface. We used SF_6 , a weakly soluble compound detectable in sea water at concentrations of 10^{-16} M (12). Time-averaged estimates of diapycnal diffusivity inferred from observations of the tracer's vertical dispersion can be compared to the more instantaneous diffusivity estimates for temperature and buoyancy deduced from microstructure data.

During a cruise of the R/V *Seward Johnson* from January to February of 1996, we occupied 75 stations with the HRP at sites ranging between the 3900-m isobath off the coast of Brazil and the western flank of the Mid-Atlantic Ridge (MAR; Fig. 1). Most of the profiles reached to within 30 m of the bottom. The resulting microstructure observations reveal a deep-ocean mixing pattern that appears to be correlated to the underlying bathymetry (Fig. 2). Above the smooth abyssal plains of the central Brazil Basin and the gradual slopes of the South American continental rise, we observed

Woods Hole Oceanographic Institution, Woods Hole, MA 02543, USA.

*To whom correspondence should be addressed. E-mail: kpolzin@whoi.edu